BOND BEHAVIOR OF GFRP BARS EMBEDDED IN FIBER REINFORCED CONCRETE

J.-Y. Lee[1*], B. Kim[1], J.-E. Kang[2], H.-Y. Choi[1]

[1]*Dept. of Architectural Engineering, Sungkyunkwan University, Suwon, Republic of Korea,*
[2]*Dept of Structural Design, ES Structural Engineering, Seoul, Republic of Korea*
** jungyoon@skku.edu*

Keywords: Glass fiber reinforced bars; structural fibers; bond behavior; interfacial bond strength, ductility

Abstract

In this study a total of 90 cubic specimens were prepared to investigate the pullout behaviours of the sand-coated and helically-wrapped GFRP bars as well as steel bars in matrix reinforced with FRC (steel, PP and PVA[a] fibers) and PVA[b]-ECC. The results of direct pull-out testing were presented and analyzed with the aim of elucidating the effect of surface treatment of bar, fiber type, and fiber volume fraction in interface and suggesting the effective evaluation method for the improved ductility. The structural fibers (steel, PP, PVA[a] fibers) and PVA[b]-ECC in the interface changed the interfacial bond behaviors, but bond failure modes largely depended on the interfacial property with the rebar. The fiber's crack closing resistance, determined by evaluating toughness indices, was used to determine optimum amount and type of fibers in the composites. The effect of concrete matrix with the structural fibers in the interface was apparent rather than that of engineering cementitious matrix with PVA[b] fibers.

1 Introduction

The application of fiber reinforced polymer (FRP) as a possible alternative for the steel rebar, especially in corrosive environment, has continuously stimulated many researchers to study bond behavior of various FRP bars in construction fields for the past two decades. The satisfactory performance of FRP bars, as a result of their non-corrosive nature and high ratio of strength to weight, has promoted their implementation in the marine environment and civil engineering community thus far [1]. The key requirement for good performance of FRP bars is the development of sufficient interfacial bond, which allows a continuous load transfer from the rebar to concrete matrix with a good failure ductility. In order to improve the bond strength of the FRP rebars, various surface treatments to FRP bars are normally performed such as the helical fiber wrapping, sand particles, deep dents, and deformations by resin [1-4]. While increased bond strength and the changes in both failure mode and failure interface location were reported with the higher concrete strength, they concluded that the pull-out mechanism of FRP bars from the concrete matrix depends on many parameters. Addition of fibers in the cement matrix has shown to enhance both the interfacial bond strength and the failure ductility of rebar embedded in the cementitious materials via the delayed crack growth and increased critical stress due to fiber bridging mechanism which reduces the stress intensity factor at the end of the crack [5]. In regard to FRP rebar, Belabi et al. [6] reported that both glass fiber reinforced polymer (GFRP) and carbon fiber reinforced polymer (CFRP) bars showed a moderate improvement in ductility response, when the concrete was reinforced with fibers, but with no distinct effect on bond strength. While the increase of bond strength due to fiber reinforcement was reported by Won et al. [7] who showed steel fibers are more effective than synthetic fibers on both the bond strength and ductility improvement.

It can be noted that researches on delaying the interfacial bond failure and producing high ductility are more appropriate rather than improving bond strength due to the unique property of fibers, though the unique mechanical properties of the interfacial region with fibers affect both the bond strength and toughness in the composites. In spite of the improved bond stress-slip curve of FRP rebars in the cementitious materials by the introduction of steel or synthetic fibers, no standard methods are available to evaluate the improved ductility in the interfacial zone. In this study, an experimental program using the two most common types of GFRP bars and three types of fibers (steel and synthetic fibers) was carried out. Herein, the results of the direct pull-out tests are presented and analyzed with the aim of elucidating the effects of the rebar surface treatment, fiber type, and fiber volume fraction and suggesting the effective measurement method for the improved ductility during post-cracking behavior.

2 Experimental program

2.1 Materials

The reinforcing bars (one type of steel bar and two types of GFRP bars used in this study) were obtained from international manufacturers. The GFRP bars were made of E-glass fibers and a thermosetting resin, and had the diameter of 12.7 mm (#4) with two different surface treatments. Herein, the GFRP bar with the sand-coated surface treatment is designated as GFRP-A and the helically-wrapped bar with sand coating as GFRP-B. The GFRP rebars with the two different surface treatments are shown in Fig. 1. Table 1 shows the material properties of the bars in detail. The types of fibers used in this study were hooked-end steel fiber, polypropylene (PP) fiber and two types of polyvinyl alcohol (PVA^a, PVA^b) fiber, and their material properties are presented in Table 2. The PVA^b fiber additionally was used in this study to evaluate the effect of matrix reinforced with engineering cementitious composites (ECC) in comparison with that of fiber-reinforced concrete. The concrete mix designs considered in this study are presented in Table 3.

Figure 1. Surface deformations and type of bars.

Rebar type	Cross setional area (mm^2)	Bar diameter (mm)	Fiber content (%)	Specific gravity (g/cm^3)	Surface treatment	Yeild strength (MPa)	Fracture strength (GPa)	Elastic modulus (GPa)
Steel	126.7	12.7	-	7.90	-	410	560	200.0
GFRP-A	129.0	12.7	70	2.04	Sand coating	-	690	42.0
GFRP-B	129.0	12.7	70	2.00	Helically wrapped	-	617	40.8

Table 1. Properties of used rebars.

Variables	PP	PVA[a]	PVA[b]	Steel
Length (mm)	30	30	8	30
Diameter (μm)	-	660	40	560
Density (g/cm^3)	0.9	1.3	1.3	7.8
Modulus (GPa)	6	29	37	200
Tensile strength (MPa)	550	800	1300	1100

Table 2. Properties of used fiber type.

Mix type	Cement (kg/m^3)	Water (kg/m^3)	Sand (kg/m^3)	Coarse aggregate (kg/m^3)	Fly ash (kg/m^3)	Fiber content (kg/m^3)	Super-plasticizer (kg/m^3)
OPC-A	394	177	697	1040	-	-	0.93
PP(0.5%)	394	177	697	1040	-	4.6	0.74
PP(1%)	394	177	697	1040	-	9.1	1.47
Steel(0.5%)	394	177	697	1040	-	40.0	0.93
Steel(1%)	394	177	697	1040	-	80.0	1.97
PVA[a](0.5%)	394	177	697	1040	-	6.5	1.47
PVA[a](1%)	394	177	697	1040	-	13.0	1.97
OPC-B	580	255	580	-	580	0	6.96
PVA[b](1%)	580	255	580	-	580	13	6.96
PVA[b](2%)	580	255	580	-	580	26	11.6

Table 3. Used mix proportion.

2.1 Test specimens

A total of 90 cubic specimens were prepared and tested. The specimen was a 190.5 × 102 × 152.4 mm^3 in size, which was modified from the specimen geometry utilized by Alavi-Fard et al. [8]. A single rebar was embedded horizontally along a central axis in each specimen as shown in Fig. 2. The bond length of the embedded rebar was set at 63.5 mm, five times the diameter of the rebar. Furthermore, in order to make an effective measurement of the interfacial bond behavior over the exact bonded length, the rebars were sheathed with soft PVC tubing before placing concrete to prevent bonding between the bar and the concrete. Concrete was placed in two layers and each layer was rodded 25 times with 16mm diameter tamping rod. The concrete was cast with the rebar in the horizontal position inside the steel formwork. After molding, the specimens were immediately covered with a plastic sheet to stop moisture loss for 24 hours. The specimens were then removed from their molds and continuously cured underwater at 21°C until the time of test. Three nominally identical specimens were prepared for each specimen type.

2.3 Test setup and testing equipment

The cubic specimen was placed on the testing machine so that the surface of the cube on the side of long end of the bar was in contact with the rigid support frame and the end of the bar was held by the jaws, with round wedges, of the testing machine as shown in Fig. 2. The pullout behaviors of the bars with and without the addition of fibers were investigated using a 2,000kN capacity universal testing machine. The bond slip between the embedded rebar and the concrete at both the loaded end and the free end were simultaneously measured using three linear variable displacement transducers (LVDTs). The readings of the applied pullout load and the corresponding three LVDTs were automatically recorded through a data logger. The compressive strength of three companion cylindrical specimens was also measured at the time of the test according to ASTM C 39 procedure [9].

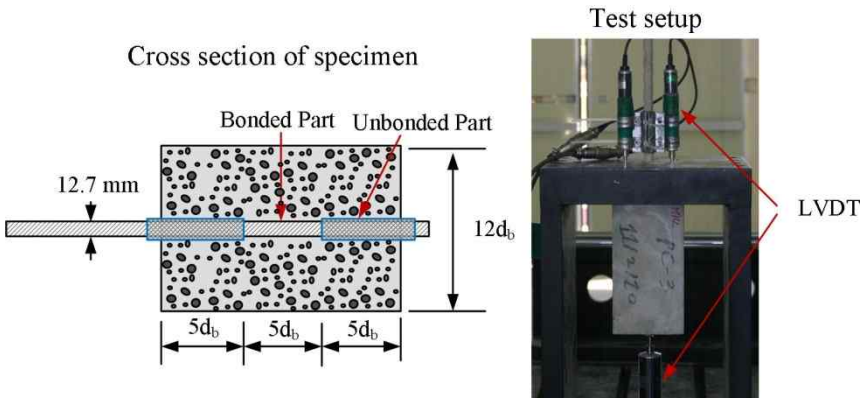

Figure 2. Specimen and setup for pullout test**.**

3 Test results

3.1 Interfacial bond property

The influence of the bar type, fiber type and fiber volume fraction on the interfacial bond behavior is investigated in this section. The contribution of steel, PP, and PVA fibers to the compressive strength in this study was not significant and other researchers [10-11] have also reported the similar results. The failure by pullout of the bars was defined when the applied load reached the maximum point. Corresponding values of maximum nominal bond stress and corresponding slip were then determined. Although the interfacial stress distribution between bar and matrix is not constant along the embedded length during the pullout test, an average bond strength was calculated as follows:

$$\tau_{max} = \frac{P_{max}}{\pi d_b l_b} \quad (1)$$

where τ_{max} is the bond strength, P_{max} is the maximum pullout load, d_b is the bar diameter, and l_b is the embedded length of the bar. The normalized bond strength was also defined to offset the effect of the compressive strength of the concrete on the bond strength evaluation of the different bar types and fiber types . The normalized or relative bond strength [12] was defined by

$$\tau_r = \frac{\tau_{max}}{\sqrt{f'_c}} \quad (2)$$

where τ_r is the normalized or relative bond strength, τ_{max} is the maximum bond strength, f'_c is the compressive strength of the concrete.

The general behavior of the interfacial bond stress vs. slip relationship is described by a sharp linear increase of the interfacial bond stress over a small range of slip and a softening of the slope was recorded due to the degradation of the interface around embedded bar. In general, the residual load-slip curves corresponding to the part of the load-slip curve beyond the first peak showed distinct characteristics with the different fiber types and the rebar types. Fig. 3 presents test results of steel bars with different types of fiber reinforcement. An almost linear behavior is observed in the ascending portion at the free-end bar, resulting in the low slips corresponding to the maximum load. The addition of hooked-end steel, PP, and PVA fibers significantly improved the maximum bond stress and residual stress subsequent to the first crack with the increase in fiber volume fraction. The typical bond stress vs. slip curves of the

sand-coated GFRP bars (GFRP-A) are shown in Fig. 4. A very sharp increase of the applied load with linear behavior at the free end bar is observed in the ascending part and an efficient load transfer with structural fibers subsequent to matrix cracking is presented during post-cracking process. Fig.5 shows the curves of the interfacial bond stress vs. slip of the helically-wrapped GFRP bars (GFRP-B). A nonlinear behavior with a gradually reduced slope was dominant in the later part of the bond strength development. As the bar is mobilized, a wedging action, which is also observed in the result of Baean et al. [13], occurs due to the sloped crushed concrete face attached to the front of the lugs for deformed and indented bars. The yield plateau observed in the curve can be attributed to the bridging effect of the fibers which effectively delays the interfacial failure process by allowing the concrete to exert an adequate confining force.

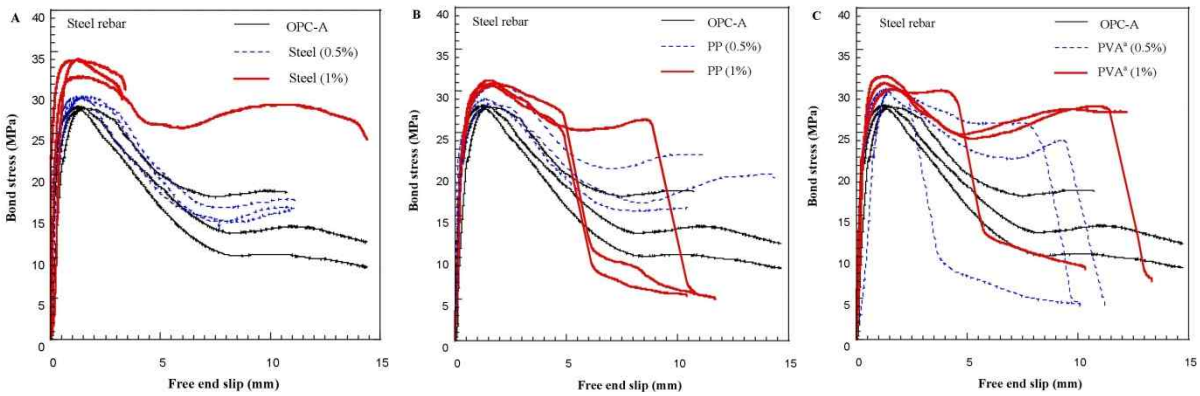

Figure 3. Bond stress vs. slip curves with steel bars: A) Steel fibers; B) PP fibers; C) PVA fibers.

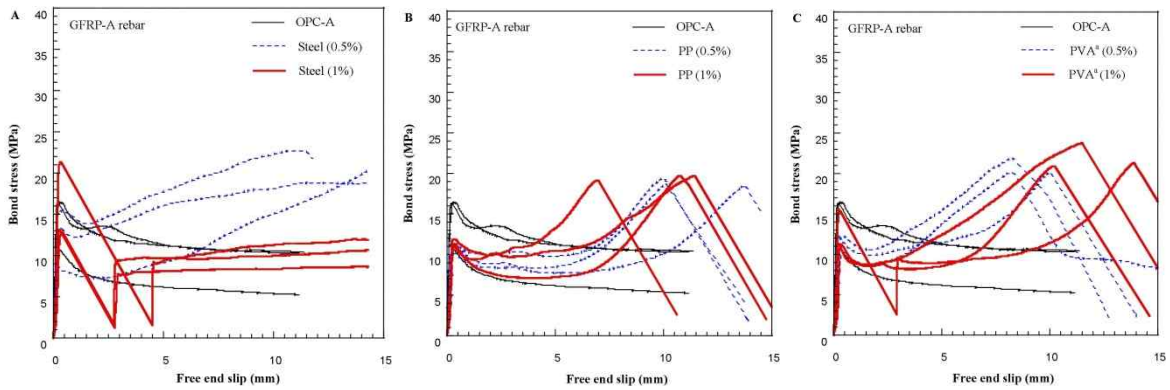

Figure 4. Bond stress vs. slip curves with GFRP-A bars: A) Steel fibers; B) PP fibers; C) PVA fibers.

For the bond behaviors of the steel, GFRP-A and GFRP-B bars reinforced with PVA^b-ECC are shown in Fig. 6. Generally, the curves are similar to those of the rebars bonded with fiber-reinforced concrete. The effect of PVA^b-ECC on the load vs. the slip curves subsequent to matrix cracking is significant rather than in the ascending curves [14]. For the steel bars, the improved bond strength and high ductile behaviors with the increase of PVA^b fiber volume fractions are observed. For the GFRP-A bars, a very sharp increase of the applied load on the free end bar is observed in the ascending part, even though the maximum bond stress was smaller than that of the steel bars. In addition, the applied load subsequent to the failure of the interface between the matrix and the rebar dropped quickly. For the GFRP-B bars, the contribution of PVA fibers subsequent to matrix cracking is apparent during the post-peak behavior.

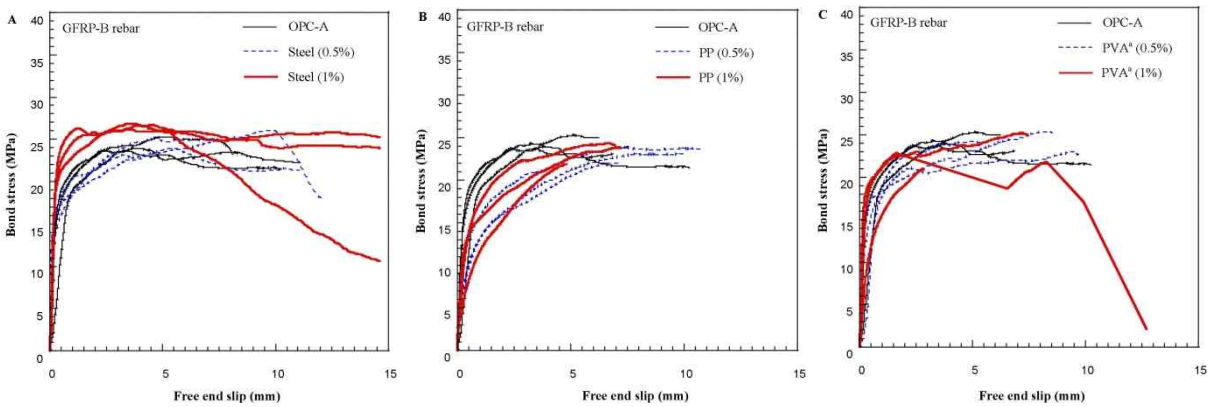

Figure 5. Bond stress vs. slip curves with GFRP-B bars: A) Steel fibers; B) PP fibers; C) PVA fibers.

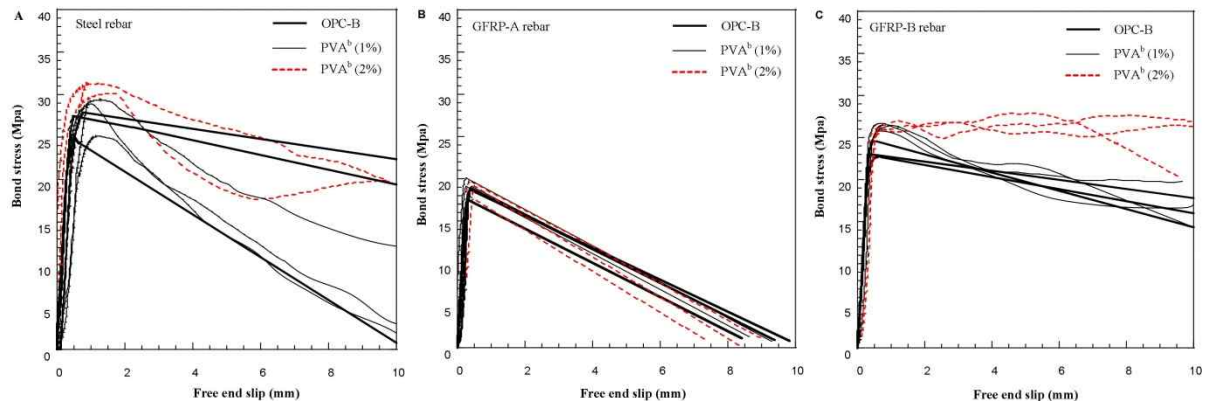

Figure 6. Bond stress vs. slip curves with PVA[b] fiber: A) Steel rebar, B) GFRP-A rebar, C) GFRP-B rebar.

For the steel bars, the addition of steel, PP, and PVA[a] fibers in concrete shows a slight increase in the relative bond strength as the fiber volume fraction increases. On the other hand, significantly improved relative bond strength was found for the helically-wrapped GFRP bars (GFRP-B) as well as sand-coated GFRP bars (GFRP-A). The difference in relative bond strength between the different fiber volume fractions is small. For the ECC, generally the addition of PVA[b] fibers increases the interfacial bond strength [14]. The contribution of PVA[b] fibers for the embedded steel bars is linearly proportional to the amount of added fibers. In comparison with the specimens with no fibers, both the GFRP-A bars and the GFRP-B bars have slightly increased bond strength, but the difference between fiber contents is negligible.

3.2 Failure modes

For the steel rebar, two different failure mechanisms exist [7]. First, the steel rebar is pulled out while the concrete between the ribs crushes and then shear cracks develop. Second, splitting failure occurs when radial stress developed by the angled faces of ribs surpasses tensile strength of concrete. The both failure modes of the steel bar in plain concrete were observed when the cubic specimens were split after the tests. The bond failure of the GFRP rebar occurs in the modes similar to those of steel rebar, and also via additional failure mechanisms due to the surface treatment of the GFRP rebar [2]. It is noted that the addition of PP, PVA[a], steel and PVA[b] fibers in concrete significantly altered the pull-out failure mechanism in the interface by delaying the crack growth and propagation [14, 15]. The interfacial failure surfaces of the rebar in the specimens reinforced with the fibers are summarized in Fig. 7.

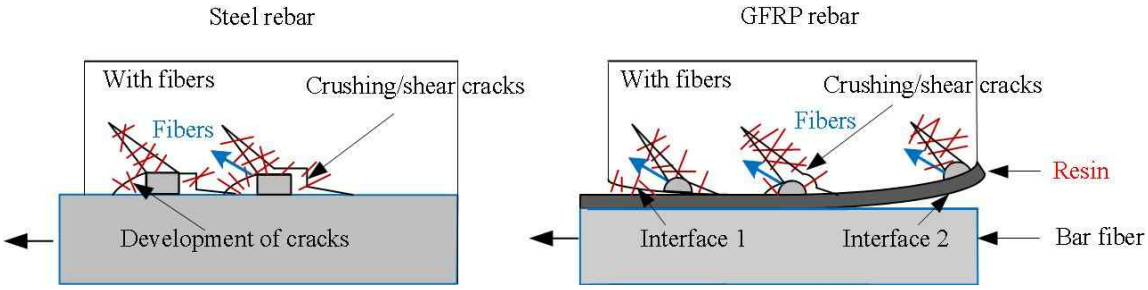

Figure 7. Idealized interfacial failure modes.

4. Effect of fiber type for ductility improvement

The contribution of the fibers ultimately resulted in the improvement of the toughness compared to the specimen with no fibers. The shape and material properties of fibers played a very important role in controlling the development of cracking. Therefore, the contribution of fibers to interfacial bond property during the crack development and propagation can be summarized as the totally dissipated bond energy and it can be evaluated by determining and evaluating toughness indices [15, 16]. The author suggests that these evaluation methods can be applied to the pullout behavior of FRP rebar for the determination of toughness and residual bond strength indices that identify the pattern of material behavior up to the selected deflection criteria. Summarized results are represented in Table 4. It is worth noting that PVA and hook end steel fibers (relatively high tensile strength, rough surface, and hydrophilic properties) have a good chemical and mechanical bonding effect to exert effective fiber-bridging closing pressures as cracks develop, and to grow and propagate in composites compared to that of the PP fibers with a relatively smooth surface structure that are hydrophobic in nature. Finally, the effect of concrete matrix with the structural fibers in the interface was apparent rather than that of engineering cementitious matrix with PVA fibers.

Mix type	Steel rebar		GFRP-A rebar		GFRP-B rebar	
	I_{s5}	I_{s10}	I_{s5}	I_{s10}	I_{s5}	I_{s10}
OPC-A	4.2	6.8	23.0	48.0	1.6	3.1
PP(0.5%)	3.7	6.4	28.7	64.9	0.6	1.4
PP(1%)	3.8	5.5	26.9	61.5	0.7	1.2
Steel(0.5%)	3.6	6.2	22.0	59.6	0.6	1.2
Steel(1%)	4.2	7.8	29.1	72.2	1.2	2.1
PVA[a](0.5%)	4.5	7.7	36.7	84.1	0.7	1.5
PVA[a](1%)	4.9	9.8	15.4	31.7	1.9	3.8
OPC-B	-	-	-	-	-	-
PVA[b](1%)	4.7	-	-	-	5.9	-
PVA[b](2%)	4.2	8.8	-	-	15.4	33.0

Table 4. Toughness index results.

5. Conclusions

The following conclusions can be drawn from the experimental results.

1. For the pull-out and residual stages, the randomly distributed fibers significantly delayed the pull-out failure of the rebars by maintaining the high residual load and toughness.
2. The addition of structural fibers changed the failure modes for GFRP bars from the partial debonding of the resin to the complete failure.

3. The fiber's crack closing resistance against the pullout of rebar was determined by evaluating toughness indices, which were useful to determine the optimum amount and type of fibers in composites.
4. Among the fibers, PVA and hook end steel fibers showed a good interfacial bonding effect to exert closing pressures of fiber bridging as cracks develop, grow and propagate, but largely depended on the bonding with surface treatment of rebars.
5. The effect of concrete matrix with the structural fibers (PP, PVA[a], steel) in the interface was apparent rather than that of engineering cementitious matrix with PVA[b] fibers.

References

[1] Rostasy FS. *FRP:The European perspective* In "Proceedings of *the First International Conference on Composites in Infrastructure*. Tuscon, Arizona, USA, (1996).
[2] Baena M, Torres L, Turon A, Barris C. Experimental study of bond behavior between concrete and FRP bars using a pull-out test*, Composite Part B: engineering,* 40, pp. 784-797 (2009).
[3] Larrade J, Silva-Rodriguez R. Bond and slip of FRP rebars in concrete. *ASCE Journal of Materials in Civil Engineering*, 5(1), pp.30-40 (1995).
[4] Lee JY, Kim TY, Kim TJ, Yi CK, Park JS, You YC, Park YH. Interfacial bond strength of glass fiber reinforced polymer bars in high-strength concrete. *Composites Part B: engineering*, 39, pp. 258-270 (2008).
[5] Li C.Y., Mobasher B. Finite element simulations of fiber pullout toughening in fiber reinforced cement based composites. *Advanced Cement Based Materials,* 7, pp. 123-132 (1998).
[6] Belabi A, Wang H. *Bond-slip response of FRP reinforcing bars in fiber reinforced concrete under direct pullout* In Proceeding *of ICFRC-international conference on fiber composites, high performance concretes and smart materials*, Chennai, India,. pp. 409-419. (2004)
[7] Won JP, Park CG, Kim HH, Lee SW, Jang CI. Effect of fibers on the bonds between FRP reinforcing bars and high –strength concrete. *Compoists Part B: engineering*, 39, pp. 749-755 (2008).
[8] Alavi-Fard M, Marzouk H. Bond behavior of high strength concrete under reversed pull-out cycle loading, *Canadian Journal of Civil Engineering,* 29, pp. 191-200 (2002).
[9] ASTM C 39/C39 M. *Standard test method for compressive strength of cylindrical concrete specimen*, Annul Book of ASTM Standards (2004).
[10] Yao W, Li J, Wu K, Mechanical properties of hybrid fiber-reinforced concrete at low fiber volume fraction, *Cement and Concrete Research* ,33, pp. 27-30 (2003).
[11] Ding Y, Kusterle W, Compressive stress-strain relationship of steel fibre-reinforced concrete at early age, *Cement and Concrete Research*, 30 pp. 1573-1579 (2000).
[12] Xial J, Falkner H. Bond behavior between recycled aggregate concrete and steel rebars. *Construction and Building Materials*, 21, pp. 395-401 (2007).
[13] Ezeldin AS, Balaguru PN, Bond behavior of normal and high-strength fiber reinforced concrete, *ACI Materials Journal*, 86(5), pp. 515-524 (Sep.-Oct. 1989)
[14] Kim B, Lee JY. Polyvinly alcohol engineering cementitious composite (PVA-ECC) for the interfacial bond behavior of glass fiber reinforced polymer bars (GFRP), *Polymers & Polymer Composites* (in printing).
[15] Kim B, Doh JH, Yi C, Lee JH. Evaluation method of structural fibers on ductility improvement of GFRP composites*, Composite Part B: engineering* (submitted).
[16] ASTM C 1018, *Standard test method for flexural toughness and first-crack strength of fiber-reinforced concrete (using beam with third-point loading),* Annual Book of ASTM Standards (1997).